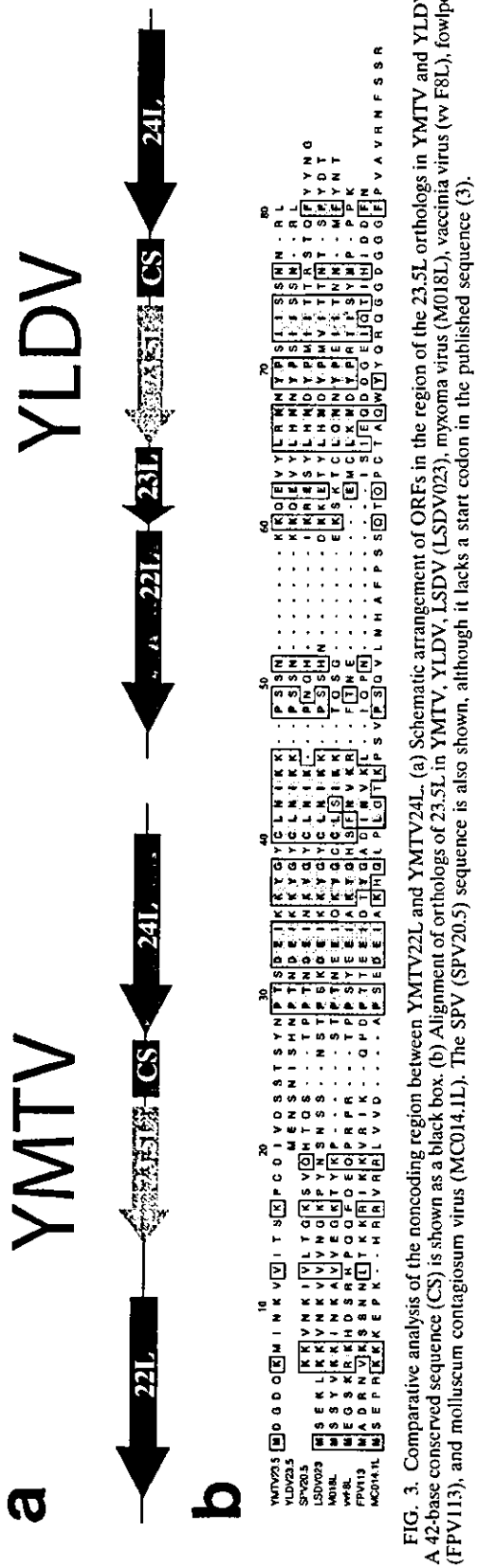

FIG. 3. Comparative analysis of the noncoding region between YMTV22L and YMTV24L. (a) Schematic arrangement of ORFs in the region of the 23.5L orthologs in YMTV and YLDV. A 42-base conserved sequence (CS) is shown as a black box. (b) Alignment of orthologs of 23.5L in YMTV, YLDV, LSDV (LSDV023), myxoma virus (M018L), vaccinia virus (vv F8L), fowlpox (FPV113), and molluscum contagiosum virus (MC014.1L). The SPV (SPV20.5) sequence is also shown, although it lacks a start codon in the published sequence (3).

either the forward (R-GFP) or the reverse complement (L-GFP) orientations in front of a promoterless GFP construct. Cells were either mock infected or infected with myxoma virus and then transfected with promoterless GFP, R-GFP, or L-GFP constructs. The L-GFP but not the R-GFP sequence was able to drive some detectable GFP expression in the absence of virus infection, but a myxoma virus coinfection greatly increased the level of expression of the L-GFP construct (Fig. 4c). From these data we conclude that the conserved sequence could act as a late promoter element for the gene 23.5L; however, other potential functions such as an involvement in viral replication or packaging cannot be excluded. The reason for the unusual conservation of this promoter sequence across four genera of poxviruses remains to be determined.

Identification of two new conserved poxvirus gene families. The central region of the poxvirus genome is inevitably enriched for genes that are highly conserved among all poxviruses. In YMTV, this conserved region maps between YMTV24L and YMTV124R. However, inspection of the genomic sequences from a number of poxviruses revealed that the region between YMTV ORFs 27L and 29L and between ORFs 120L and 121L were unexpectedly divergent (Fig. 5a). Analysis of the region between YMTV27L and YMTV29L identified an ORF, designated 28.5L, which encodes a 58-amino-acid protein (Table 1). Initially we examined the region between 27L and 29L in YLDV, where the previously assigned 28R gene is present. Analysis of the YLDV sequence revealed a clear ortholog of 28.5L (Fig. 6a) which overlaps extensively with 28R. Based on the fact that there are no other reported poxvirus versions of YLDV 28R in the database and there is typically only minor overlap of poxvirus ORFs with each other, we postulate that 28.5L represents the true yatapox virus ORF that maps between 27L and 29L for both YMTV and YLDV and that the slightly longer 28R encoded in the opposite polarity originally annotated for YLDV might not be expressed.

Since 28.5L appeared to be present in both sequenced members of the *Yatapoxvirus* genus, we examined members of other poxvirus genera to determine if orthologs of this gene could be identified. We examined the noncoding sequence between the orthologs of 27L and 29L in myxoma virus, SPV, LSDV, vaccinia virus, molluscum contagiosum virus, and fowlpox virus to determine if a previously unreported version of 28.5L existed in these genomes. Surprisingly, we found closely related orthologs of 28.5L in all poxvirus species examined, with the exception of fowlpox virus (Fig. 5b and 6b). Interestingly, the deduced ortholog of 23.5L in myxoma virus overlaps extensively with M024R (which bears no similarity with YLDV 28R [Fig. 6a]). This conservation of 23.5L in so many poxvirus genera and the lack of any other orthologs for M024R has led us to conclude that M23.5L, rather than the annotated M024R (8), may be the correct ORF that maps between M023L and M025L.

We next examined the 199-bp noncoding region between YMTV ORFs 120L and 121L. A single 44-amino-acid ORF designated YMTV120.5L was identified which lacked sequence similarity to any gene in the published database. Therefore, as in the case of the gap between 27L and 29L of YMTV, we examined the sequence gap between YMTV120L and YMTV121L (Fig. 5a) and looked for other poxvirus ORFs in this conserved region. This approach yielded clear orthologs of

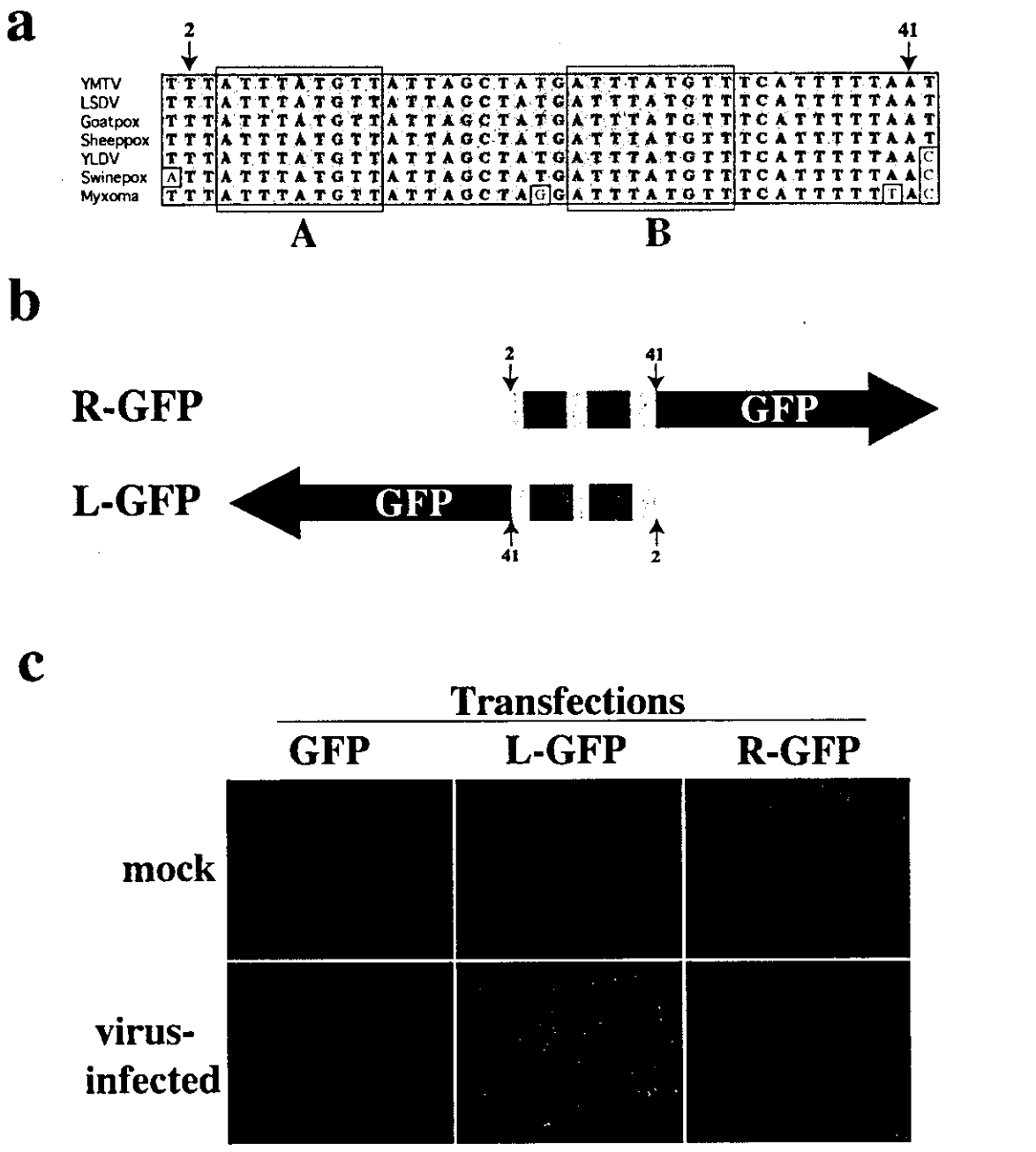

FIG. 4. Analysis of the conserved promoter-like sequence between YMTV23.5L and YMTV24L. (a) Alignment of a conserved sequence found between orthologs of YMTV23.5L and YMTV24L. The sequence within the red boxes labeled "A" and "B" represents the 9-bp repeat. The numbers above the grey box indicate the nucleotide positions. (b) Schematic of the orientation of the promoterless GFP with respect to the orientation of the cloned myxoma virus conserved sequence. R-GFP contains the conserved sequence from bases 2 to 41. L-GFP contains the reverse complement of the conserved sequence. The red boxes show the location of the two repeats in panel a. (c) Cells were either mock infected or infected with myxoma virus and subsequently transfected with either a promoterless GFP, R-GFP, or L-GFP construct. Forty-eight hours postinfection, the cells were visualized using a fluorescence microscope.

YMTV120.5L in all poxvirus species examined (Fig. 5b and 6c). Interestingly, versions of YMTV120.5L were previously identified in myxoma virus and molluscum contagiosum virus, although originally no relationship was reported between them, presumably because the small gene size made determination of significant identity difficult. However, the position of the conserved ORF in the genomes, the sequence similarities, and the similar gene sizes all indicate that these ORFs are part

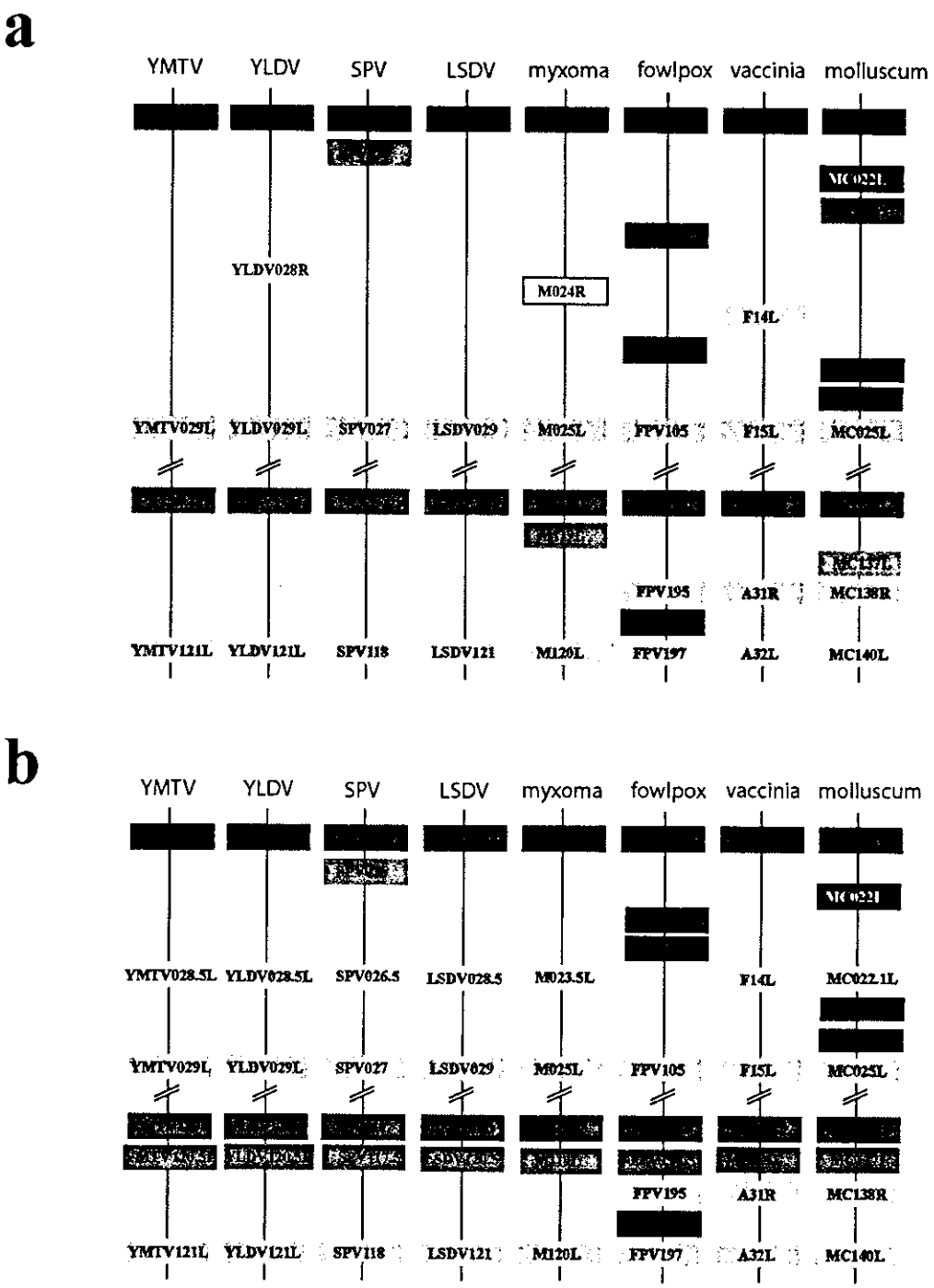

FIG. 5. Alignment of two conserved ORF clusters in a variety of poxvirus genera. (a) Alignment of predicted ORFs from representative members from seven of the eight poxvirus genera. Two regions of the genome are shown, the orthologous region between YMTV027L and YMTV029L and the region between YMTV120L and YMTV121L. Orthologous ORFs share the same color. (b) Analysis of the region between YMTV027L/029L and YMTV120L/121L revealed two new conserved gene families. The proposed arrangements of these ORFs are shown, highlighting the arrangement of the two new gene families YMTV028.5L and YMTV120.5L.

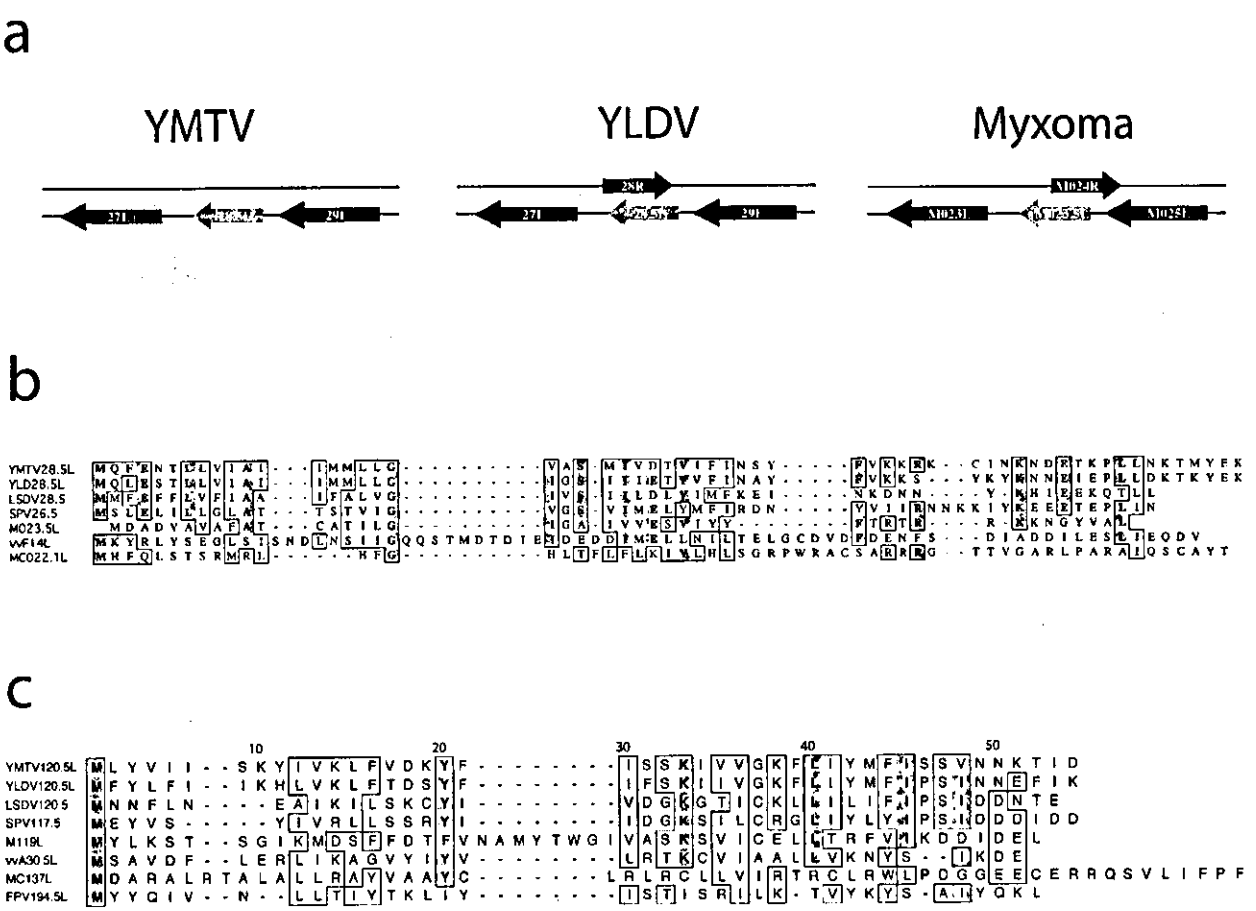

FIG. 6. Alignments of the predicted YMTV28.5L and YMTV120.5L protein families. (a) Arrangement of YMTV 28.5L orthologs in YMTV, YLDV, and myxoma virus. (b) Alignment of orthologs of YMTV28.5L, including YLDV28.5L, LSDV (LSDV28.5), myxoma virus (M023.5L), vaccinia virus (vvF14L), SPV (SPV26.5), and molluscum contagiosum virus (MC022.1L). (c) Alignment of orthologs of YMTV120.5L, including YLDV120.5L, LSDV (LSDV120.5), myxoma virus (M119L), vaccinia virus (vvA30.5L), swinepox virus (SPV117.5), fowlpox virus (FPV194.5L), and molluscum contagiosum virus (MC137L).

of an ancestrally evolved gene cluster that is conserved across multiple poxvirus genera.

DISCUSSION

In this work we report the complete sequence of the YMTV genome and have identified three ORFs previously unidentified in most poxviruses. The YMTV genome size of 134,721 bases represents the smallest poxvirus genome yet sequenced. In contrast, the closely related YLDV genome is approximately 144,575 bases long (15). The difference in genome sizes between YMTV and YLDV is due to the complete deletion of 13 ORFs found in YLDV but absent from YMTV. The bulk of the YMTV deleted ORFs are found at the left end of the genome and represent determinants of immune evasion, host range, or genes of unknown function (Table 2). Clinically, YMTV and YLDV produce distinct diseases, with YMTV producing histiocyte-filled tumors upon infection, whereas YLDV infection resembles a mild form of smallpox (5, 20, 27). It is possible that the absence of various YLDV gene products might, in some way, contribute to the tumorigenic phenotype produced upon YMTV infection, but the contribution of these 13 deleted genes to disease phenotype awaits further study.

The data presented here highlight the utility of using a comparative genomic approach when analyzing viral genomes for predicted genes. One of the difficulties in whether to assign a nucleotide sequence as an annotated ORF, particularly for small ORFs of less than 150 nucleotides, is that there is no way to confirm that a predicted ORF is actually expressed until the translated protein or mRNA is detected experimentally. However, we reasoned that if a putative ORF actually encodes a protein, it would be conserved in at least some other poxvirus genus members. Therefore, we examined the tentatively assigned noncoding regions between ORFs in poxvirus genomic sequences to identify yatapoxvirus ORFs with demonstrable similarity in terms of size, sequence, and presence of contiguous orthologs. This approach identified three new yatapoxvirus gene families (23.5L, 28.5L, and 120.5L) that are clearly conserved throughout many genera of poxviruses (Table 3). These three gene families all appear to encode unique proteins with no significant similarity with any other viral or cellular proteins

TABLE 3. Members of three new poxvirus gene families

Virus	YMTV23.5 family			YMTV28.5 family			YMTV120.5 family		
	Gene	Start	Stop	Gene	Start	Stop	Gene	Start	Stop
YMTV	23.5L	14742	14530	28.5L	20085	19909	120.5L	107287	107421
YLDV	23.5L	17960	17808	28.5L	23539	23366	120.5L	113015	112881
SPV	20.5	13430	13229	26.5	20113	19949	117.5	110742	110617
LSDV	023	15949	15734	28.5	22161	22012	120.5	112519	112394
Goatpox virus strain G20-LKV	023	15430	15211	28.5	21620	21470	120.5	111927	111807
Sheeppox virus	023	15557	15342	28.5	21685	21536	120.5	112134	112009
Myxoma virus	018L	18513	18316	23.5L	23834	23703	119L	114993	114844
Shope fibroma virus	018L	17726	17526	23.5L	23037	22906	119L	114122	114003
Vaccinia virus									
Ankara	037L	30731	30534	044L	37105	36884	141.5L	133014	132889
Tian Tan	TF8L	35166	35318	TF14L	41537	41758	TA30.5L	141666	141540
Copenhagen	F8L	38878	38684	F14L	45318	45100	A30.5L	141046	140918
WR	VACWR047	35577	35774	VACWR053	41967	42188	VACWR153.5	142061	141933
Variola virus									
Garcia	E8L	27400	27579	E14L	33818	34039	A34.5L	133824	133696
Bangladesh 1975	C12L	27031	27228	C18L	33457	33678	A33.5L	133432	133313
India 1967	E8L	27597	27400	E14L	34039	33818	A33.5L	132818	132690
Ectromelia virus	EVM031	44331	44528	EVM037	50749	50964	132.5	150491	150363
Camelpox virus	CMLV043	38437	38634	CMLV049	44853	45074	CMLV170.5	144313	144185
Monkeypox virus	C14L	36022	35828	C20L	42461	42240	A31.5L	141603	141484
Cowpox virus	CPXV055	52234	52431	CPXV062	58648	58869	CPVX165.5	159066	158938
Fowlpox virus	113	134861	135058				194.5L	227787	227667
Molluscum contagiosum virus	014.1L	18646	18897	MC22.1L	28628	28807	137L	158648	158812

in the sequence database, but which are clearly conserved in most of the known poxvirus genera. With the renewed interest in variola virus, the causative agent of smallpox, it is particularly relevant to identify new families of conserved viral genes that may have important conserved roles in poxvirus replication or pathogenesis.

An unexpected finding from these observations was that several small ORFs that turned out to be members of conserved poxvirus gene families were originally characterized as unique. For example, fowlpox virus gene FPV113 (2) and molluscum contagiosum virus gene MC014.1L (23) were identified as unique genes, but our comparative analysis demonstrated that they are instead part of a larger poxvirus gene family that includes the vaccinia virus F8L gene. The reason that FPV113 and MC014.1L were not identified as being related to vaccinia virus F8L was likely that it is difficult to reach a level of statistical significance with computer database searches when the raw similarity score is reduced because of their small sizes.

Comparing genomic sequences from different poxviruses in this fashion can provide insight into the evolutionary history of these viruses. For example, comparing the presumptive noncoding regions of both YLDV and YMTV with the same region of SPV revealed a potential pseudogene in YLDV and YMTV that had significant sequence similarity with the SPV002 gene. The presence of the same pseudogene in both YMTV and YLDV but of a functional copy of the gene in SPV implies that the pseudogene arose after the split of the suipox viruses from the yatapox viruses. In this way, we can develop an evolutionary timeline for some of the major events that differentiated members of the diverse poxvirus genera.

In addition to the identification of potential ORFs, the comparative genomic approach resulted in the unexpected identification of a 40-nucleotide stretch of YMTV sequence that was 100% conserved across members of the *Yatapoxvirus*, *Suipoxvirus*, and *Capripoxvirus* genera. This domain represents the most highly conserved sequence yet described among these poxviruses. Even the highly conserved concatemer resolution sequence, which is involved in the essential elements of poxvirus replication at the termini, is only 81% conserved between these species. This conserved sequence maps in the noncoding region between YMTV ORFs 23.5L and 24L. Although we demonstrated that this sequence can function as a late promoter element (Fig. 4), it is not yet clear if that is the actual function of this sequence during a viral infection. For example, the poxvirus concatemer resolution sequence can function as a poxvirus late promoter element (TAAAT) sequence (28); however, its primary role appears to be in resolving concatemers during viral replication (19). One way to test the potential function of this conserved promoter-like sequence would be to generate virus deletion mutants in any one of the virus members that contain a copy of the sequence.

The data presented here have illustrated some of the potential applications of taking a comparative approach to analyze poxvirus genomics. Through the comparison of poxvirus genomes across genera we identified three new gene families that had previously been overlooked because of their small size. In addition, conserved sequences that do not encode an ORF but that potentially play an important role in poxvirus replication were also identified. The comparative genomic analysis that we undertook was originally made possible due to the sequencing of the YMTV genome and the ability to compare its sequence to that of another relatively close species, YLDV (15). However, in theory, the comparative approach that we took could be applied to any viral family and may be particularly valuable when trying to

predict whether small potential ORFs truly encode a protein.

ACKNOWLEDGMENTS

We thank Karim Essani and Koji Ishii for critical reading of the manuscript.

This work was supported by the National Cancer Institute of Canada and by Viron Therapeutics, Inc.

REFERENCES

1. **Afonso, C., E. Tulman, Z. Lu, L. Zsak, N. Sandybaev, U. Kerembekova, V. Zaitsev, G. Kutish, and D. Rock.** 2002. The genome of camelpox virus. Virology **295**:1–9.
2. **Afonso, C. L., E. R. Tulman, Z. Lu, L. Zsak, G. F. Kutish, and D. L. Rock.** 2000. The genome of fowlpox virus. J. Virol. **74**:3815–3831.
3. **Afonso, C. L., E. R. Tulman, Z. Lu, L. Zsak, F. A. Osorio, C. Balinsky, G. F. Kutish, and D. L. Rock.** 2002. The genome of swinepox virus. J. Virol. **76**:783–790.
4. **Amano, H., Y. Ueda, and T. Miyamura.** 1995. Identification and characterization of the thymidine kinase gene of Yaba virus. J. Gen. Virol. **76**:1109–1115.
5. **Ambrus, J. L., E. T. Feltz, J. T. Grace, Jr., and G. Owens.** 1963. A virus-induced tumor in primates. Natl. Cancer Inst. Monogr. **10**:447–458.
6. **Antoine, G., F. Scheiflinger, F. Dorner, and F. G. Falkner.** 1998. The complete genomic sequence of the modified vaccinia Ankara strain: comparison with other orthopoxviruses. Virology **244**:365–395.
7. **Bearcroft, W. G. C., and M. F. Jamieson.** 1958. An outbreak of subcutaneous tumours in rhesus monkeys. Nature **182**:195–196.
8. **Cameron, C., S. Hota-Mitchell, L. Chen, J. Barrett, J.-X. Cao, C. Macaulay, D. Willer, D. Evans, and G. McFadden.** 1999. The complete DNA sequence of myxoma virus. Virology **264**:298–318.
9. **Davison, A. J., and B. Moss.** 1989. Structure of vaccinia virus late promoters. J. Mol. Biol. **210**:771–784.
10. **Downie, A. W., and C. Espana.** 1972. Comparison of Tanapox virus and Yaba-like viruses causing epidemic disease in monkeys. J. Hyg. **70**:23–32.
11. **Goebel, S. J., G. P. Johnson, M. E. Perkus, S. W. Davis, J. P. Winslow, and E. Paoletti.** 1990. The complete DNA sequence of vaccinia virus. Virology **179**:247–266.
12. **Grace, T. T. J., and E. A. Mirand.** 1963. Human susceptibility to a simian tumor virus. Ann. N. Y. Acad. Sci. **108**:1123–1128.
13. **Johnson, G. P., S. J. Goebel, and E. Paoletti.** 1993. An update on the vaccinia virus genome. Virology **196**:381–401.
14. **Knight, J. C., F. J. Novembre, D. R. Brown, C. S. Goldsmith, and J. J. Esposito.** 1989. Studies on Tanapox virus. Virology **172**:116–124.
15. **Lee, H.-J., K. Essani, and G. L. Smith.** 2001. The genome sequence of Yaba-like disease virus, a Yatapoxvirus. Virology **281**:170–192.
16. **Massung, R. F., L. I. Liu, J. Qi, J. C. Knight, T. E. Yuran, A. R. Kerlavage, J. M. Parsons, J. C. Venter, and J. J. Esposito.** 1994. Analysis of the complete genome of smallpox variola major virus strain Bangladesh-1975. Virology **201**:215–240.
17. **McNulty, W. P., W. C. Lobitz, F. Hu, C. A. Maruffo, and A. S. Hall.** 1968. A pox disease in monkeys transmitted to man. Clinical and histological features. Arch. Dermatol. **97**:286–293.
18. **Merchlinsky, M., and B. Moss.** 1989. Nucleotide sequence required for resolution of the concatemer junction of vaccinia virus DNA. J. Virol. **63**: 4354–4361.
19. **Moss, B.** 2001. *Poxviridae*: the viruses and their replication, p. 2849–2883. *In* D. M. Knipe and P. M. Howley (ed.), Fields virology, 4th ed., vol. 2. Lippincott Williams & Wilkins, Philadelphia, Pa.
20. **Niven, J. S. F., J. A. Armstrong, C. H. Andrews, H. G. Pereira, and R. C. Valentine.** 1961. Subcutaneous 'growths' in monkeys produced by a poxvirus. J. Pathol. Bacteriol. **81**:1–14.
21. **Sanger, F., S. Nicklen, and A. R. Coulson.** 1977. DNA sequencing with chain-terminating inhibitors. Proc. Natl. Acad. Sci. USA **93**:5463–5467.
22. **Seet, B. T., J. B. Johnston, C. R. Brunetti, J. W. Barrett, H. Everett, C. Cameron, J. Sypula, S. Nazarian, A. Lucas, and G. McFadden.** 2003. Poxviruses and immune evasion. Annu. Rev. Immunol. **21**:377–423.
23. **Senkevich, T. G., E. V. Koonin, J. J. Bugert, G. Darai, and B. Moss.** 1997. The genome of molluscum contagiosum virus: analysis and comparison with other poxviruses. Virology **233**:19–42.
24. **Shchelkunov, S. N., R. F. Massung, and J. J. Esposito.** 1995. Comparison of the genome DNA sequences of Bangladesh-1975 and India-1967 variola viruses. Virus Res. **36**:107–118.
25. **Shchelkunov, S. N., A. V. Totmenin, V. N. Loparev, P. F. Safronov, V. V. Gutorov, V. E. Chizhikov, J. C. Knight, J. M. Parsons, R. F. Massung, and J. J. Esposito.** 2000. Alastrim smallpox variola minor virus genome DNA sequences. Virology **266**:361–386.
26. **Shchelkunov, S. N., A. V. Totmenin, P. F. Safronov, M. V. Mikheev, V. V. Gutorov, O. I. Ryazankina, N. A. Petrov, I. V. Babkin, E. A. Uvarova, L. S. Sandakhchiev, J. R. Sisler, J. J. Esposito, I. K. Damon, P. B. Jahrling, and B. Moss.** 2002. Analysis of the monkeypox virus genome. Virology **297**:172–194.
27. **Sproul, E. E., R. S. Metzgar, and J. T. J. Grace.** 1963. The pathogenesis of Yaba virus-induced histiocytomas in primates. Cancer Res. **23**:671–675.
28. **Stuart, D., K. Graham, M. Schreiber, C. Macaulay, and G. McFadden.** 1991. The target DNA sequence for resolution of poxvirus replicative intermediates is an active late promoter. J. Virol. **65**:61–70.
29. **Tulman, E. R., C. L. Afonso, Z. Lu, L. Zsak, G. F. Kutish, and D. L. Rock.** 2001. Genome of lumpy skin disease virus. J. Virol. **75**:7122–7130.
30. **Tulman, E. R., C. L. Afonso, Z. Lu, L. Zsak, J.-H. Sur, N. T. Sandybaev, U. Z. Kerembekova, V. L. Zaitsev, G. F. Kutish, and D. L. Rock.** 2002. The genomes of sheeppox and goatpox viruses. J. Virol. **76**:6054–6061.
31. **Willer, D., G. McFadden, and D. H. Evans.** 1999. The complete genome sequence of Shope (rabbit) fibroma virus. Virology **264**:319–343.

ACADEMIC PRESS

Available online at www.sciencedirect.com

SCIENCE DIRECT®

Virology 314 (2003) 16–25

VIROLOGY

www.elsevier.com/locate/yviro

Production and release of infectious hepatitis C virus from human liver cell cultures in the three-dimensional radial-flow bioreactor

Hideki Aizaki,[a] Seishi Nagamori,[b,*] Mami Matsuda,[a] Hayato Kawakami,[c] Osamu Hashimoto,[d] Hiroaki Ishiko,[d] Masaaki Kawada,[e] Tomokazu Matsuura,[f] Satoshi Hasumura,[e] Yoshiharu Matsuura,[g] Tetsuro Suzuki,[a] and Tatsuo Miyamura[a]

[a] *Department of Virology II, National Institute of Infectious Diseases, Shinjuku-ku, Tokyo 162-8640, Japan*
[b] *Department of Pharmacology and Toxicology, Kyorin University School of Medicine, Mitaka, Tokyo 181-8611, Japan*
[c] *Department of Anatomy, Kyorin University School of Medicine, Mitaka, Tokyo 181-8611, Japan*
[d] *Mitsubishi Kagaku Bio-clinical Laboratories, Inc., Itabashi-ku, Tokyo 174-0056, Japan*
[e] *Kiba Hospital, Koutou-ku, Tokyo 135-0042, Japan*
[f] *Department of Laboratory Medicine, The Jikei University School of Medicine, Minato-ku, Tokyo 105-8461, Japan*
[g] *Research Center for Emerging Infectious Diseases, Research Institute for Microbial Diseases, Osaka University, Suita, Osaka 565-0871, Japan*

Received 5 February 2003; returned to author for revision 19 March 2003; accepted 22 April 2003

Abstract

Lack of efficient culture systems for hepatitis C virus (HCV) has been a major obstacle in HCV research. Human liver cells grown in a three-dimensional radial-flow bioreactor were successfully infected following inoculation with plasma from an HCV carrier. Subsequent detection of increased HCV RNA suggested viral replication. Furthermore, transfection of HCV RNA transcribed from full-length cDNA also resulted in the production and release of HCV virions into supernatant. Infectivity was shown by successful secondary passage to a new culture. Introduction of mutations in RNA helicase and polymerase regions of HCV cDNA abolished virus replication, indicating that reverse genetics of this system is possible. The ability to replicate and detect the extracellular release of HCV might provide clues with regard to the persistent nature of HCV infection. It will also accelerate research into the pathogenicity of HCV, as well as the development of prophylactic agents and new therapy.

Keywords: HCV; Three-dimensional radial-flow bioreactor; Replication; Full-length cDNA; Infectious clone; Particles; Reverse genetics; Infection; In vitro culture model; Artificial liver

Introduction

More than 100 million people are infected with hepatitis C virus (HCV) worldwide, and many are prone to developing chronic hepatitis with subsequent cirrhosis and hepatocellular carcinoma (HCC) (Choo et al., 1989; Kuo et al., 1989; Saito et al., 1990). Measures to eliminate HCV from carriers before progressive and degenerative liver diseases develop are needed. However, studies aimed at elucidating the mechanism behind persistent HCV infection have been hampered by lack of an efficient in vitro culture system capable of supporting viral replication.

Many attempts have been made to culture HCV in vitro. However, to date, only limited HCV replication was suggested by reverse transcription-polymerase chain reaction (RT-PCR) techniques, and HCV-specific proteins were not generally detected (Ito et al., 2001; Kato and Shimotohno, 1999; Thomson and Liang, 2000). Infectious cDNA clones have been successfully developed for positive-sense RNA viruses (Boyer and Haenni, 1994). Full-length HCV cDNA clones have also been successfully used to infect chimpanzees in in vivo transfection experiments (Kolykhalov et al., 1997, 2000; Yanagi et al., 1997). Furthermore, replication of genome-length dicistronic HCV RNA was shown in a

* Corresponding author. Fax: +81-3-5285-1161.
E-mail address: nagamori@ma.rosenet.ne.jp

0042-6822/03/$ – see front matter © 2003 Elsevier Inc. All rights reserved.
doi:10.1016/S0042-6822(03)00383-0

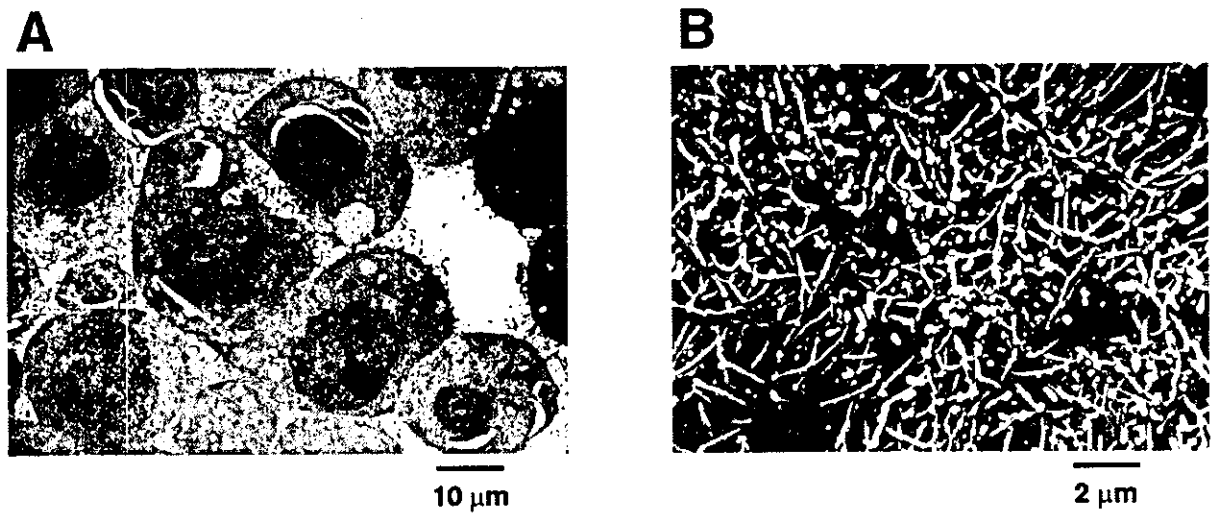

Fig. 1. FLC4 cells in the RFB. (A) Transmission electron micrograph image of FLC4 cells cultured in the RFB. Scale bar shows 10 μm. (B) Scanning electron micrographs showing FLC4 cells attached with the RFB matrix. Scale bar shows (B).

human liver cell line when HCV RNA was dicistronically transfected together with selective markers (Ikeda et al., 2002; Pietschmann et al., 2002). Although replication of the entire HCV genome was also observed, any infectious HCV virions could not be detected (Pietschmann et al., 2002). Thus, viral RNA replication and synthesis of fully processed viral proteins may not be sufficient to produce infectious virus. One or more host factor(s) provided only by permissive cells may be required for the assembly of infectious virions. Alternatively, monolayer cultures of mammalian cells, typically human liver-derived cell lines, may not permit the assembly and release of HCV from cells.

Nagamori et al. established a three-dimensional (3D) radial-flow bioreactor (RFB) system, in which human liver cells retained their differentiated hepatocyte functions and morphological appearance for an extended period of time (Kawada et al., 1998). This system was originally designed to develop artificial liver tissue (Kawada et al., 1998; Matsuura et al., 1998). However, in this study, we utilized the system to examine cells transfected with full-length HCV RNA or inoculated with infectious serum. Although the titer was not particularly high, propagation of HCV in vitro was clearly shown. Furthermore, infectious virus was released into the supernatant in the absence of obvious cell lysis.

Results

FLC4 cell culture in RFB system

We found that cells from a human hepatocellular carcinoma-derived cell line, FLC4 (Functional Liver Cell 4) (Aoki et al., 1998), produced albumin at a rate of 18 $\mu g/10^5$ cells/day, when cultured in the RFB system. In conventional monolayer cultures, FLC4 cells produced albumin at a rate of 2.5 $\mu g/10^5$ cells/day.

α-Fetoprotein production by FLC4 cells also differed among the two culture systems (7 $\mu g/10^5$ cells/day were produced by cells in the RFB system versus an undetectable amount by cells in the monolayer culture). Production of albumin and α-fetoprotein by FLC4 cells in the RFB culture continued for more than 100 days without cell passage, during which time the temperature was reduced from 37 to 32°C, causing a gradual increase in oxygen consumption.

Transmission electron microscopy (TEM) has shown maintenance of tight junctions among RFB-cultured FLC4 cells and normal intercellular spaces (Fig.1A). Scanning electron microscopy (SEM) has shown that, unlike FLC4 cells in monolayer cultures, FLC4 cells cultured in the RFB system retain structurally intact microvilli on their surface (Fig. 1B). RFB culture is therefore thought to provide an environment in which the natural architecture and function of cells are maintained. We tested the replication of HCV under these conditions as a model of HCV replication in vivo.

Infection experiments

First, we inoculated FLC4 cells with infectious human plasma in RFB culture. The infectious plasma (no. 6) was derived from a healthy HCV carrier and its infectivity was eventually proven after posttransfusion hepatitis C was observed in a patient that had received the carrier's blood (Takeuchi et al., 1990; Aizaki et al., 1998). Afterward, the infectivity of the carrier's plasma was tested by inoculation of chimpanzees, and its titer was determined to be $10^{5.5}$ chimpanzee infectious doses per milliliter (Sugitani and Shikata, 1998).

Table 1
HCV infection of FLC4 cells cultured in the RFB following inoculation with the plasma

Days	HCV RNA[a] (log_{10} copies/ml)	ALT (IU/l)
−2	−	7
0[b]	5	2
1	+	NT[c]
2	−	NT
3	−	2
4	−	NT
5	−	2
7	−	NT
9	−	2
11	−	NT
12	−	2
14	−	NT
16	+	2
19	4–5	2
23	4	2
26	+	2

[a] HCV RNA in the culture fluids was determined by qualitative and quantitative RT-PCR. Log of copy numbers identified by the quantitative assay are shown. +, positive by the qualitative assay but below the detection limit (10^3 copies/ml) by the quantitative one. −, negative by both of assays.
[b] On the day 0, plasma no. 6 was inoculated.
[c] NT, not tested.

After cells (1×10^9) were inoculated with 1 ml of the plasma in RFB culture by infusion, HCV RNA was detected by PCR in the culture fluid for 2 days. This was thought to be due to residual virus following the infusion. RNA was not detected in the culture fluid for the next 2 weeks (less than 50 copies/ml). HCV RNA was then detected on day 16 postinfection (p.i.) and reached $10^4 - 10^5$ copies/ml by days 19 and 23 p.i. (Table 1). After this, HCV RNA was detected in the culture fluid for more than 80 days by the qualitative assay (data not shown). Subsequent experimentation using the same cells and inoculum reproduced this profile of HCV RNA detection in the culture fluid (data not shown). In this experiment, the cells were harvested on day 14, and further culture was discontinued. Intracellular HCV core protein levels were as high as 75 pg/mg of total cellular protein in the cells. Although the precise number of cells supporting virus replication could not be determined, this level of core protein expression is almost equivalent to that observed in the liver tissue of chronic hepatitis C patients (Koike et al., 2002).

The hypervariable regions (HVR) of HCV RNA detected on day 23 p.i. were compared to those of plasma no. 6 (Table 2). Plasma no. 6 (donor plasma) was found to contain a mixture of clones with different HVR sequences, but more than half of these contained A1 sequences (Sugitani and Shikata, 1998). After transmission, these mixed clones converged until one clone was primarily detected (clone A1) in infected chimpanzees (Chimp.) (Sugitani and Shikata, 1998), and in the human hepatitis patient, who received no. 6 plasma for transfusion (Recip.) (Aizaki et al., 1998). Interestingly, of the 20 clones tested in this RFB culture study, 19 had A1 clone sequences. These data suggest that the HCV RNA detected was not that of the infused virus but, rather, it appears that the RFB culture selectively supported the replication of certain clones. Clones having A1 sequences may have a replication advantage in RFB culture.

Table 2
Comparison of amino acid sequences of HVR among HCV clones derived from plasma no. 6

Species	Sequence of HVR[a]	Number of clones			
		Donor[b]	Chimp.	Recip.	RFB
	384 410				
A1	H Y R V T R G V Q G H V T S T L T S L F R P G A S Q K	11	20	2	19
A2	S -[c]	1	0	0	0[c]
A3	- L - - -	1	0	0	0
A4	- F - -	0	0	0	1
B1	N - H -	1	0	0	0
B2	N - H - - - A - - - - G A F G - - - - - Q - - - - - -	3	0	0	0
B3	N - H - - - A - - - - G A F - - - - - - T S - - - - -	0	0	1	0
B4	D - H - - - A - - - - G A F - - - - - - T S - - - - -	3	0	0	0
B5	D - H - - - A - - - - G A F Q - - - - - T S - - - - -	0	0	1	0
B6	D - H - - - A - - - - G A F Q - - - - - T S - - - - R	0	0	1	0
B7	D - H - - - A - - - - G A F H - - - - - T S - - - - -	0	0	2	0
B8	D - H - - - A - - C - G A F H - - - - - T S - - - - -	0	0	1	0
C1	N - H - - - - - - - R - A - K - - - F - T - - P - - -	0	0	1	0
D1	- - H - - - - - - - - - - - - - - - F K - S - - - - -	0	0	1	0
		20	20	10	20

[a] Sequences of HVR in HCV clones recovered from the culture fluid of the RFB (RFB), the plasmas of a donor (Donor), a chimpanzee (Chimp.), and a recipient (Recip.) are shown.
[b] The sequences and diversity in Donor, Chimp., and Recip. are from Sugitani and Shikata (1998), and Aizaki et al. (1998).
[c] Dashes represent amino acid residues identical to the clone A-1.

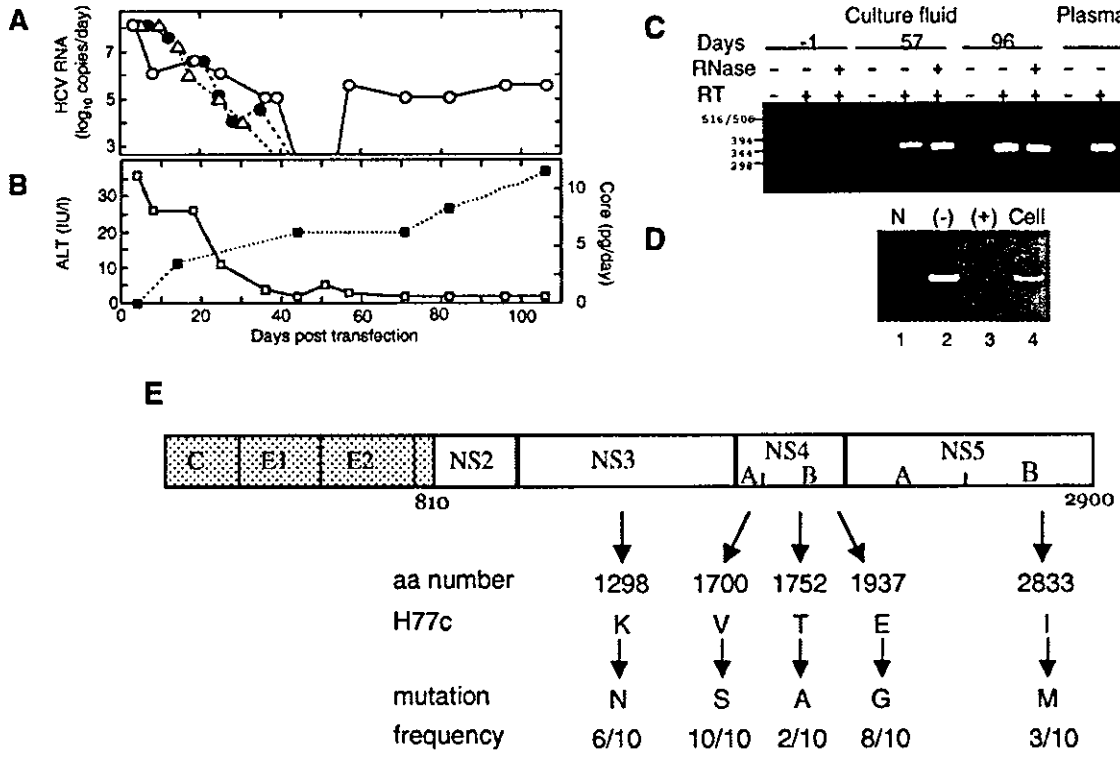

Fig. 2. HCV propagation in FLC4 cells in RFB culture following transfection with the RNA derived from the infectious cDNA clone. (A) HCV RNA titers in the culture fluid after transfection of the infectious HCV RNA H77c (○), helicase inactive mutant RNA H77cHel- (△), and RdRp inactive mutant RNA H77cRdRp- (●). On the day 0, the full-length HCV RNA H77c was transfected. HCV RNAs at days 44, 47, 51, and 54 were positive, but their RNA titers were $<10^1$ copies/ml. (B) ALT levels (□) and the amount of HCV core protein (■) in the culture fluid after transfection of H77c, respectively. (C) Culture fluids of the H77c transfectant were treated with (+) or without (−) RNase A. Samples were then amplified by RT-PCR with (+) or without (−) enzyme in the RT step. The culture fluids collected on day −1, 57, and 96 after inoculation, patient plasma, and the cell-culture medium added with 6×10^4 molecules of HCV RNA transcript were analyzed. (D) Negative-strand-specific RT-PCR, Lane 1, cellular RNA without added synthetic RNA. Lanes 2 and 3, with added synthetic negative (−) and positive (+)-strand RNA, respectively. Lane 4, cellular RNA from the cells harvested on the day 110 p.t. (E) HCV clones recovered from the culture fluids of the RFB. (Top) Schematic presentation of the complete HCV genome. The ORF with the structural proteins (shaded box) located in the amino-terminal portion of polyprotein, and the remainder encodes the nonstructural protein (NS2 to NS5B). (Middle) The positions and frequencies. Overlapping RT-PCR products were sequenced and the mutations observed in nonstructural protein regions are illustrated, along with the frequency with each arose. The amino acid number is indicated above the H77c sequence.

Transfection experiments

The above results suggest that RFB culture supports the replication and release of HCV in culture fluid. To confirm this, we transfected cells in RFB culture with HCV RNA. RNA derived from an infectious full-length HCV cDNA clone (H77c) (Yanagi et al., 1997) was used. This clone was derived from HCV genotype 1a and was proven infectious by direct inoculation into chimpanzee livers.

Cells were transfected with HCV RNA and cultured using the RFB system. HCV RNA was assayed by RT-PCR using samples of culture fluid. As in the infection experiments described above, the amount of viral RNA in the culture fluid declined immediately after transfection. At days 44, 47, 51, and 54 posttransfection (p.t.), HCV RNA was positive by the qualitative assay but below the detection limit (10^3 copies/day) by the quantitative one (Aizaki et al., 1998). However, the sample collected on day 57 p.t. indicated HCV RNA levels as 10^5 – 10^6 copies/day. This level remained here for 100 days of culture (Fig. 2A, open circles and solid line). In addition, HCV core protein gradually increased in the culture fluid until a maximum level of approximately 13.2 pg/day was reached on day 106 p.t. (Fig. 2B, filled squares and dotted line). The relative amounts of HCV core protein (13.2 pg/day) and HCV RNA (10^5 – 10^6 copies/day) detected on day 106 p.t. are consistent with previously reported data on native HCV virions (Kashiwakuma et al., 1996). Since ALT levels did not increase within the culture fluid (Fig. 2B, open squares and solid line), direct hepatocyte injury did not appear to result from HCV replication.

To determine whether the HCV RNA detected was packaged within virions, the culture fluid collected on days 57 and 96 p.t. was treated with RNase and examined by quantitative RT-PCR. As shown in Fig. 2C, the HCV nucleic acid was first confirmed to be RNA. However, the RNA was RNase resistant, suggesting that it is contained within virions. The RNase resistance might also indicate HCV RNA of

the double-stranded replicative form. Nevertheless, such RNA, if any, trapped in membranous structures of the cells may not be conferred resistance to nucleases. In the RFB system, RNase-resistant HCV RNA was not detected after transfection of mutant clones (described later). Furthermore, in cells harvested on day 110 p.t., negative-strand HCV RNA was detected by tagged RT-PCR (Fig. 2D).

To verify that this system supports the replication of transfected HCV RNA, we constructed two mutated full-length HCV RNAs, termed H77cHel− and H77cRdRp−, containing lethal mutations of helicase and polymerase, respectively. After transfection, the residual RNA of these mutant clones gradually declined in the culture fluid, and no RNA was detected by RT-PCR after day 38 and 40 p.t., for H77cHel− and H77cRdRp−, respectively (Fig. 2A, H77cHel−: open triangles; H77cRdRp−: filled circles). Thus the detection of HCV RNA 44 days after transfection of wild-type HCV RNA must have been due to actual viral replication.

To confirm HCV replication and to determine whether mutations arose during the course of the study, we determined the nucleotide sequences of entire nonstructural regions of the clone detected on day 110 p.t. and compared them with the original clone (Fig. 2E). We observed 43 substitution mutations, all of which resulted in amino acid changes. This is not derived from RT errors during RT-PCR amplification because similar sequence changes were seen in the independent RT-PCR reaction. In particular, mutations of V1700S in the NS4A, E1937G in the NS4B, and K1298N in the NS3 regions were frequently observed (in 60% or more of the sequenced clones), which suggests that these mutations might enhance RNA replication within the FLC4-RFB system. We are now analyzing whether or not transcripts with these mutations enhance infectivity or have a replication advantage in RFB culture.

Late-stage culture fluid (80 to 110 days posttransfection) was collected, concentrated, and examined by TEM. A number of spherical particles, between 30 and 80 nm in diameter, were observed, and probably represent two entities of approximately 30 and 60 nm in size (Fig. 3A). The suspension was then fractionated by spinning within a continuous 10–60% (w/w) sucrose gradient. The fractions were then treated with Triton X-100/NaOH/polyethylene glycol and assayed for HCV core protein. The core protein was detected in both 1.07 and 1.20 g/ml fractions, while HCV RNA was predominantly detected in fractions of 1.03–1.09 g/ml (Fig. 3B). Although quantitative assays to detect HCV envelope proteins have not been developed, the lower density fraction observed in this study (1.03–1.09 g/ml) might reflect the presence of HCV particles (1.03–1.12 g/ml), as previously observed in the serum of hepatitis C patients (Kanto et al., 1994; Kaito et al., 1994). The higher density fraction, in contrast, may represent empty particles without RNA. To distinguish between the particles observed in these fractions, an indirect immunogold electron microscopic study was carried out (Figs. 3C and D). Spherical virus-like particles, 55 to 60 nm in diameter, in the 1.07 g/ml fraction reacted with monoclonal antibody to HCV E1 protein. We did not observe any specific reactions of concentrated supernatant from transfected cells with anti-Histidine antibody (Fig. 3E).

The secondary passage

The virus particle-containing supernatant collected at days 93, 94, and 95 p.t. was pooled and transferred to a fresh RFB culture of FLC4 cells. No HCV RNA was detected in supernatant collected at days 1–16 p.i. However, HCV RNA was detected on day 18, 24, and 28 p.i. The HVR sequences of this HCV RNA were mostly (90%) A1 clone sequences. New clones with a single base change were detected after another 14 days. In addition, HCV core protein was detected in the culture fluid on day 24 and 28 p.i. (Table 3). These results further suggest that HCV is produced in RFB culture and that released HCV is infectious.

Discussion

Despite numerous efforts to grow HCV, full replication of HCV has not been achieved in conventional monolayer cultures using any type of cell (Kato and Shimotohno, 1999; Thomson and Liang, 2000). Even when HCV RNA is detected by PCR in monolayer cultures, synthesis of newly synthesized HCV-specific proteins is not observed (Bartenschlager and Lohmann, 2001). A robust and reliable cell-culture system by which to grow HCV is urgently needed (Randall and Rice, 2001).

Recent reports have demonstrated HCV replication in human hepatocytes following transplantation into mice (Ilan et al., 2002; Mercer et al., 2001). This model provided a useful system to evaluate anti-HCV agents. However, researchers have yet to isolate infectious HCV virions.

In this connotation, the establishment of a HCV replication system (engineered HCV minigenomes) has been a real breakthrough in recent HCV research (Lohmann et al., 1999; Blight et al., 2000). This has also made reverse genetic HCV research possible. Furthermore, the ability to passage these cells has revealed that clones with "adaptive" mutations eventually become dominant (Blight et al., 2000; Lohmann et al., 2001; Krieger et al., 2001). However, the consensus sequences responsible for enhancement of HCV RNA replication have not been identified, even after examinations of the same clone (type 1b) and hepatocyte cell line (Huh-7 cells). This system was first developed to replicate only the nonstructural region of HCV genome, but further developed to enable replication of the full-length HCV genome. Although HCV RNA was synthesized, along with all properly processed HCV proteins, infectious virions were not produced (Ikeda et al., 2002; Pietschmann et al., 2002). Host cell factor(s) essential for virus assembly and release might not be provided, even by Huh-7 cells, which

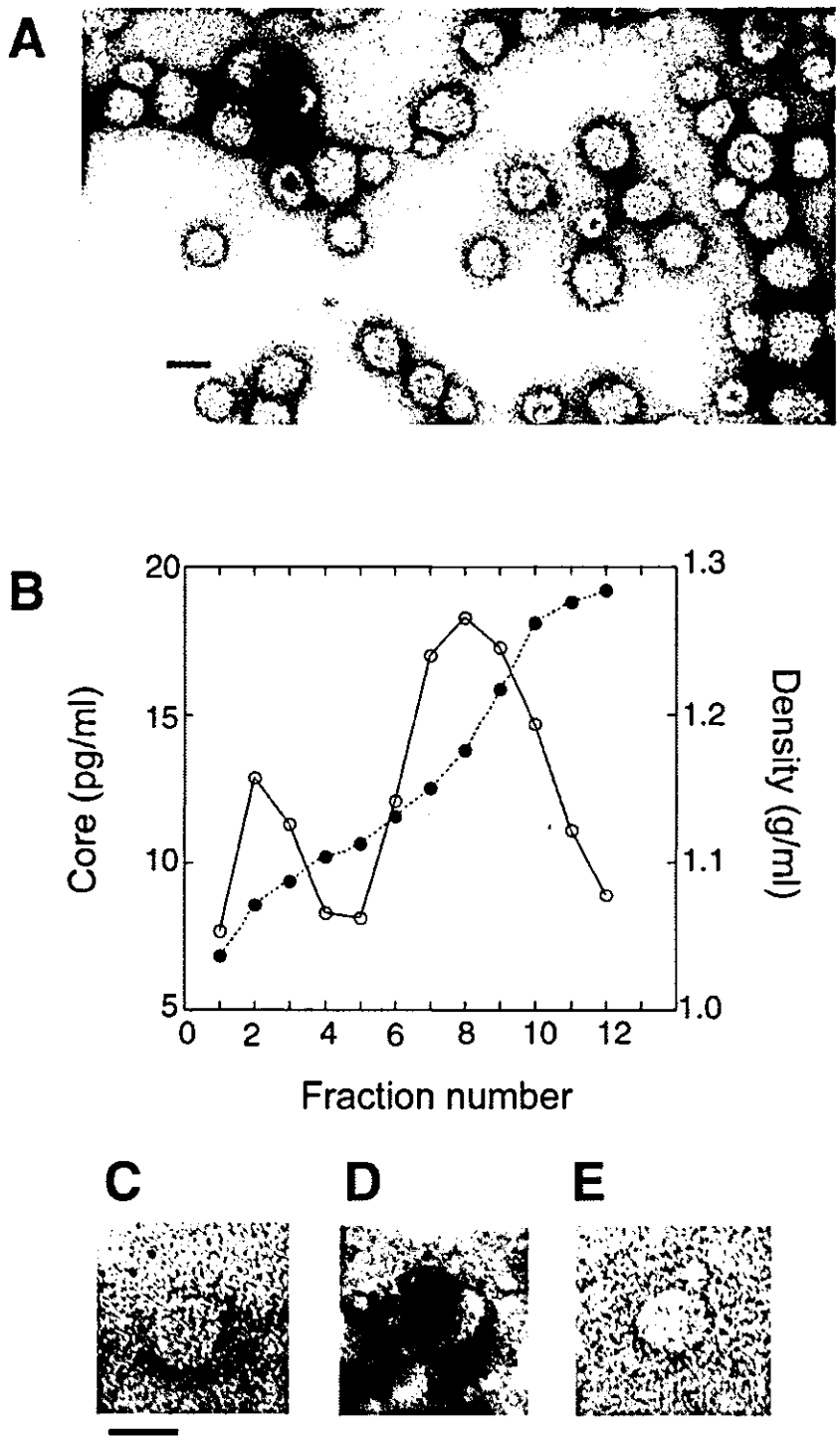

Fig. 3. Analysis of HCV-like particles in culture medium. (A) Culture fluid of the H77c transfectant was concentrated, stained with uranyl acetate, and examined by TEM. (B) HCV core protein in fractions from sucrose density gradient centrifugation. Amounts of HCV core protein (○) and buoyant densities (●) are shown. (C, D, E) Immunoelectron microscopy of the particles purified by sucrose gradient centrifugation. (C, D) Virus-like particles reacted with mouse monoclonal antibody against HCV E1 protein at a dilution of 1:10, and their antibody haloes were identified by binding to goat anti-mouse IgG-conjugated colloidal gold particles (6 nm) at a dilution of 1:20. (E) Control reaction using mouse monoclonal antibody against histidine residues antigen. The scale bars represent 50 nm.

Table 3
Secondary passage of HCV produced from the viral RNA transfection in the RFB culture

Days	HCV RNA[a]	Core[b] (pg/day)
−2	−	0
0[c]	+	5.3
1	+	2.1
3	−	0
5	−	0
7	−	0
9	−	0
11	−	0
13	−	0
16	−	0
18	+	0
20	−	0
22	−	0
24	+	6.9
28	+	14.5

[a] HCV RNA was detected qualitatively by RT-PCR (positive, +; negative, −).
[b] Core antigen was measured by the EIA method.
[c] Supernatant fluid of the RFB culture transfected with HCV RNA was transferred to new FLC4 cells in the RFB on day 0.

are capable of hosting viral RNA replication and HCV protein synthesis.

The results presented in this article clearly indicate that HCV replicates in FLC4 cells in the RFB system. In this study, we repeated the infection, transfection, and secondary passage experiments three times and obtained reproducible results. We also performed a mock-infected RFB culture for 4 months, during which time culture supernatant was harvested every week and examined for HCV RNA and HCV core protein. Negative results were obtained for both (data not shown).

In the culture medium of FLC4 cells in RFB culture, 10^6 – 10^7 copies/day of HCV were detected 2–3 weeks after infection, and 10^5 – 10^6 copies/day were detected 2–4 months after transfection. Although the viral growth of HCV in culture remains inefficient compared to that of other known viruses, this is the first report to unequivocally demonstrate HCV replication in tissue culture, as well as the production of infectious HCV derived from full-length HCV RNA.

The reason for different profiles of detection of HCV RNA and core protein is unclear (Fig. 2B). It is possible that the two assays have different sensitivities. Differences in the half-lives of viral RNA and HCV core protein may be also explain the difference. Nonetheless, the slow but gradual increase in HCV RNA and core protein observed in this study excludes the possibility that the results are due to HCV contamination or detection of the originally infused HCV RNA. These results also suggest that selection of clones capable of viral replication occurs during FLC4/RFB culture. Furthermore, it was shown that the viral quasispecies have changed before and after passages. Efforts to select clones with adaptive mutations enhancing both RNA replication and the production of infectious progeny are ongoing.

The key point of this work is the RFB culture, which allows liver cells to maintain their physiological function for a long time in culture. The RFB is a vertically extended cylindrical matrix with porous bead microcarriers having a honeycomb-like structure. This structure enables contact between cells and circulating components, including oxygen and nutrients, without excessive shear stress. The RFB has an effective air space ratio of 50%; thus, the microcarriers have much of their surface area exposed, which supports the long-term viability of the cells in culture. Cells cultured in the RFB system maintain their polarity within a well-defined 3D structure, having tight intercellular junctions and close connectivity with other epithelial cell membranes. These characteristics are important for the sustained function of liver cells in culture, including secretory and endocytic/transcytotic hepatocyte pathways.

A number of enveloped viruses have been reported to mature at distinct membrane domains within monolayers of polarized epithelial cells. For example, paramyxoviruses and orthomyxoviruses bud from the apical surface, while rhabdoviruses, retroviruses, and baculoviruses bud from a basolateral domain (Boulan and Sabatini, 1978). Similarly, FLC4 cells in the RFB are thought to maintain their polarity in a well-defined 3D structure, which is necessary for the replication and secretion of HCV.

The use of FLC4 cells may contribute to the success of this system. We have previously shown that this cell line supports efficient HCV structural gene expression by a recombinant adenovirus vector (Aoki et al., 1998). The results of this report also suggest that some host factors which increase the efficiency of translation of HCV minigene RNA are present in FLC4, but not other cells, including several commonly used human hepatoma cell lines. Furthermore, using a cell fusion assay, we recently found that FLC4 cells exhibit a high affinity for cell fusion with CHO cells expressing HCV envelope proteins on their surface (Takikawa et al., 2000). However, FLC4 cells in conventional monolayer cultures were not observed to support HCV replication following infection with no. 6 plasma. Although a small amount of virus was detected by PCR on day 19 p.i., less than 1 to 10–100th of the amount of virus per cell obtained with RFB culture was observed (data not shown). HCV RNA was not detected beyond day 19 p.i.

We are now attempting to simplify the method of RFB culture, by culturing fewer cells to better monitor HCV replication and intracellular events. In the immediate future, we will attempt to confirm the infectivity of HCV isolated from RFB culture by inoculation of chimpanzees. In addition, we would like to study the intracellular localization of processed HCV proteins, as well as virus assembly and the effects of specific antibodies and inhibitors. All of these things need to be done. Nevertheless, the evidence of infectivity of HCV RNA shown in the present work illustrates the potential of reverse genetics to delineate the mechanism

of HCV replication at a molecular level. This system will no doubt prove quite useful for studying the mechanism of persistent HCV infection and to evaluate the efficacy of vaccines, as well as various HCV specific inhibitors.

Materials and methods

Inoculum

We used plasma (no. 6) from a donor known to carry infectious HCV. Competitive RT-PCR detected 10^5 genome/ml of HCV RNA in the plasma (Sugitani and Shikata, 1998). pCV-H77C, which contains a full-length cDNA clone of strain H77 of HCV, was kindly provided by Dr. J. Bukh, National Institutes of Health, USA (Yanagi et al., 1997). We also constructed two full-length mutant clones (H77cHel- and H77cRdRp-) of HCV, containing D1316A (4286 to 4289), and G2737A (8551 to 8552), D2738A (8554), and D2739G (8557 to 8559) substitutions, respectively (Kolykhalov et al., 2000).

RFB culture of FLC4 cells

We developed a RFB culture system (Able, Japan) (Kawada et al., 1998; Matsuura et al., 1998) of FLC4 cells, produced from the cloning of JHH4 cells, in an attempt to maintain hepatocyte function in culture for an extended period of time. The RFB system, having an area of 2.7 m^2, was seeded with 1×10^9 FLC4 cells. Culture medium containing 2% FCS was added at a flow rate of 50 ml/day. To monitor the viability of cells, oxygen and glucose consumption, as well as albumin secretion, were continuously monitored throughout the duration of the study. The culture temperature was reduced from 37 to 35°C immediately following inoculation with plasma, and again to 32°C on day 51 p.i. to maintain continual slow growth of cells. As a consequence, oxygen consumption increased steadily, reaching 250 mg/day by day 30 p.i. and 350 mg/day by day 70 p.i. Despite the effects of low temperature on the culture, albumin secretion remained above 75 μg/ml throughout the culture period of 100 days.

Infection and transfection

In the infection experiments, FLC4 cells were seeded in the RFB and cultured in ASF medium (Ajinomoto, Tokyo, Japan), containing 2% fetal calf serum, at a flow rate of 100 ml/day. One milliliter of plasma no. 6 was added, after which HCV RNA and ALT levels were measured in the culture fluid. To maintain an oxygen concentration of less than 1.0 ppm at the RFB outlet during culture, the culture temperature was gradually reduced from 37 to 32°C.

In the transfection experiments, serum-free ASF medium was added to FLC4 cells in RFB culture at a rate of 50 ml/day. pCV-H77C, pCV-H77cHel-, or pCV-H77cHel- was linealized with *Xba*I, and 10 μg of each RNA transcript was mixed with lipofectin (Invitrogen, Carlsbad, CA) and diluted with 10 ml of Opti-MEM (Invitrogen). The mixture was then used to inoculate cells in the RFB.

For secondary passage, supernatant was collected on days 93, 94, and 95 p.t. (pooled to approximately 150 ml) and frozen at −80°C, until which time it was thawed and centrifuged at 8000 *g* for 15 min. After this, the supernatant, containing approximately 1.5×10^6 copies of HCV, was transferred to new FLC4 cells in RFB culture. Fifty milliliters of culture fluid was collected every day and replaced with 50 ml of new, fresh medium.

Analysis and quantitation of HCV RNA

HCV RNA in the medium was qualitatively detected by RT-PCR as described previously (Aizaki et al., 1998). Quantitative determination of HCV RNA was performed according to the competitive PCR method described by Kaneko et al. (1992). The limit of detection for HCV RNA by quantitative PCR was 10^3 copies/ml (Aizaki et al., 1998). RT-PCR was performed independently in two different laboratories (National Institute of Infectious Diseases and Mitsubishi Kagaku Bio-clinical Laboratories, Japan), and the same results were obtained. The nucleotide and amino acid sequences of HVRs of HCV envelope glycoprotein E2 were compared. Treatment with RNase was done as described previously by Kolykhalov et al. (1997). Negative-stranded HCV RNA was detected by strand-specific PCR as described previously by Lanford et al. (1994). Synthetic positive-and negative-strand RNAs encompassing the 5′ untranslated region of HCV were prepared by in vitro transcription using T7 RNA polymerase, followed by extensive purification with DNase to remove DNA. The purified RNAs were mixed with cellular RNA from FLC4 to mimic the conditions of transfected cells and to check for the generation of false positives by PCR. PCR products from one round of amplification were analyzed by agarose gel electrophoresis.

Enzyme immunoassay for HCV core antigen

The culture medium was centrifuged at 8000 *g* for 90 min, after which the supernatant was centrifuged at 100,000 *g* for 3 h. The precipitates were suspended in lysis buffer (Promega, Madison, WI) and HCV core antigen was measured using the highly sensitive enzyme immunoassay (EIA) method (Kashiwakuma et al., 1996).

Electron microscopy study

Cell samples for TEM and SEM were prepared as described previously (Kawada et al., 1998). Briefly, FLC4 cells in RFB culture were fixed in 2.5% glutaraldehyde in 0.1 M phosphate buffer (pH 7.4). After treatment with 0.1% osmium tetroxide in the same buffer, specimens were de-

hydrated in ethanol, after which they were embedded in a mixture of propyloxide and EPOK812 epoxy resin. Thin sections were examined with a transmission electron microscope (JEOL DEM1200-EX, Nihon Denshi Co., Japan). FLC4 cells attached to microcarriers were fixed to the observation table and dehydrated, after which they were submerged in 100% isoamine acetate. Samples coated with carbon and gold were observed with a scanning electron microscope (JEOL-35CF, Nihon Denshi Co.).

To analyze the virus-like particles, culture fluid of cells transfected with HCV RNA was collected and concentrated by ultracentrifugation. The pellet obtained by centrifugation was suspended in 1.5 ml of ASF medium and one-third of the suspension was reconcentrated. After this, the resultant pellet was suspended in 3 μl of ASF medium and applied to a formvar-carbon grid for negative staining. For IEM study, mouse monoclonal antibody against HCV E1 protein (1:10 dilution) and goat anti-mouse IgG-conjugated colloidal gold particles (6 nm; 1:20 dilution) were used as first and second antibodies, respectively.

Acknowledgments

We thank Drs. J. Bukh and R. Purcell for providing a full-length HCV cDNA. This work was supported by Grants-in-Aid from the Second-Term Comprehensive 10-Year Strategy for Cancer Control, Research on Advanced Medical Technology, Research on Emerging and Re-emerging Infectious Diseases from the Ministry of Health and Welfare, the Organization for Pharmaceutical Safety and Research, Japan, and the Promotion and Mutual Aid Corporation for Private Schools of Japan.

References

Aizaki, H., Aoki, Y., Harada, T., Ishii, K., Suzuki, T., Nagamori, S., Toda, G., Matsuura, Y., Miyamura, T., 1998. Full-length complementary DNA of hepatitis C virus genome from an infectious blood sample. Hepatology 27, 621–627.

Aoki, Y., Aizaki, H., Shimoike, T., Tani, H., Ishii, K., Saito, I., Matsuura, Y., Miyamura, T., 1998. A human liver cell line exhibits efficient translation of HCV RNAs produced by a recombinant adenovirus expressing T7 RNA polymerase. Virology 250, 140–150.

Bartenschlager, R., Lohmann, V., 2001. Novel cell culture systems for the hepatitis C virus. Antiviral Res. 52, 1–17.

Blight, K.J., Kolykhalov, A.A., Rice, C.M., 2000. Efficient initiation of HCV RNA replication in cell culture. Science 290, 1972–1974.

Boulan, E.R., Sabatini, D.D., 1978. Asymmetric budding of viruses in epithelial monolayers: a model system for study of epithelial polarity. Proc. Natl. Acad. Sci. USA 75, 5071–5075.

Boyer, J.C., Haenni, A.L., 1994. Infectious transcripts and cDNA clones of RNA viruses. Virology 198, 415–426.

Choo, Q.-L., Kuo, G., Weiner, A.J., Overby, L.R., Bradley, D.W., Houghton, M., 1989. Isolation of a cDNA clone derived from a blood-borne non-A, non-B viral hepatitis genome. Science 244, 359–362.

Ikeda, M., Yi, M.-K., Li, K., Lemon, S.M., 2002. Selectable subgenomic and genome-length dicistronic RNAs derived from an infectious molecular clone of the HCV-N strain of hepatitis C virus replicate efficiently in cultured Huh7 cells. J. Virol. 76, 2997–3006.

Ilan, E., Arazi, J., Nussbaum, O., Zauberman, A., Eren, R., Lubin, I., Neville, L., Ben-Moshe, O., Kischitzky, A., Litchi, A., Margalit, I., Gopher, J., Mounir, S., Cai, W., Daudi, N., Eid, A., Jurim, O., Czerniak, A., Galun, E., Dagan, S., 2002. The hepatitis C virus (HCV)-trimera mouse: a model for evaluation of agents against HCV. J. Infect. Dis. 185, 153–161.

Ito, T., Yasui, K., Mukaigawa, J., Katsume, A., Kohara, M., Mitamura, K., 2001. Acquisition of susceptibility to hepatitis C virus replication in HepG2 cells by fusion with primary human hepatocytes: establishment of a quantitative assay for hepatitis C virus infectivity in a cell culture system. Hepatology 34, 566–72.

Kaito, M., Wastanabe, S., Tsukiyama-Kohara, K., Yamaguchi, K., Kobayashi, Y., Konishi, M., Yokoi, M., Ishida, S., Suzuki, S., Kohara, M., 1994. Hepatitis C virus particle detected by immunoelectron microscopic study. J. Gen. Virol. 75, 1755–1760.

Kaneko, S., Murakami, S., Unoura, M., Kobayashi, K., 1992. Quantitation of hepatitis C virus RNA by competitive polymerase chain reaction. J. Med. Virol. 37, 278–282.

Kanto, T., Hayashi, N., Takehara, T., Hagiwara, H., Mita, E., Naito, M., Kasahara, A., Fusamoto, H., Kamada, T., 1994. Buoyant density of hepatitis C virus recovered from infected hosts: two different features in sucrose equilibrium density-gradient centrifugation related to degree of liver inflammation. Hepatology 19, 296–302.

Kashiwakuma, T., Hasegawa, A., Kajita, T., Takata, A., Mori, H., Ohta, Y., Tanaka, E., Kiyosawa, K., Tanaka, T., Tanaka, S., Hattori, N., Kohara, M., 1996. Detection of hepatitis C virus specific core protein in serum of patients by a sensitive fluorescence enzyme immunoassay (FEIA). J. Immunol. Methods 190, 79–89.

Kato, N., Shimotohno, K., 1999. Systems to culture hepatitis C virus, in: Hagedorn, C.H., Rice, C.M. (Eds.), The Hepatitis C Viruses, Springer, Berlin, pp. 261–278.

Kawada, M., Nagamori, S., Aizaki, H., Fukaya, K., Niiya, M., Matsuura, T., Sujino, H., Hasumura, S., Yashida, H., Mizutani, S., Ikenaga, H., 1998. Massive culture of human liver cancer cells in a newly developed radial flow bioreactor system: ultrafine structure of functionally enhanced hepatocarcinoma cell lines. In Vitro Cell. Dev. Biol. Anim. 34, 109–115.

Koike, K., Tsutsumi, T., Fujie, H., Shintani, Y., Kyoji, M., 2002. Molecular mechanism of viral hepatocarcinogenesis. Oncology 62, 29–37.

Kolykhalov, A.A., Agapov, E.V., Blight, K.J., Mihalik, K., Feinstone, S.M., Rice, C.M., 1997. Transmission of hepatitis C by intrahepatic inoculation with transcibed RNA. Science 277, 570–574.

Kolykhalov, A.A., Mihalik, K., Feinstone, S.M., Rice, C.M., 2000. Hepatitis C virus-encoded enzymatic activities and conserved RNA elements in the 3′ nontranslated region are essential for virus replication in vivo. J. Virol. 74, 2046–2051.

Krieger, N., Lohmann, V., Bartenschlager, R., 2001. Enhancement of hepatitis C virus RNA replication by cell culture-adaptive mutations. J. Virol. 75, 4614–4624.

Kuo, G., Choo, Q.-L., Alter, H.J., Gitnick, G.L., Redeker, A.G., Purcell, R.H., Miyamura, T., Dienstag, J.L., Alter, M.J., Stevens, C.E., Tegtmeier, G.E., Bonino, F., Colombo, M., Lee, W.-S., Kuo, C., Berger, K., Shuster, F.R., Overby, L.R., Bradley, D.W., Houghton, M., 1989. An assay for circulating antibodies to a major etiologic virus of human non-A, non-B hepatitis. Science 244, 362–364.

Lanford, R.E., Sureau, C., Jacob, J.R., White, R., Fuerst, T.R., 1994. Demonstration of in vitro infection of chimpanzee hepatocytes with hepatitis C virus using strand-specific RT/PCR. Virology 202, 606–614.

Lohmann, V., Korner, F., Dobierzewska, A., Bartenschlager, R., 2001. Mutations in hepatitis C virus RNAs conferring cell culture adaptation. J. Virol. 75, 1437–1449.

Lohmann, V., Korner, F., Koch, J., Herian, U., Theilmann, L., Bartenschlager, R., 1999. Replication of subgenomic hepatitis C virus RNAs in a hepatoma cell line. Science 285, 110–113.

Matsuura, T., Kawada, M., Hasumura, S., Nagamori, S., Obata, T., Yamaguchi, M., Hataba, Y., Tanaka, H., Shimizu, H., Unemura, Y., Nonaka, K., Iwaki, T., Kojima, S., Aizaki, H., Mizutani, S., Ikenaga, H., 1998. High density culture of immortalized liver endothelial cells in the radial-flow bioreactor in the development of an artificial liver. Int. J. Artif. Organs 21, 229–234.

Mercer, D.F., Schiller, D.E., Elliott, J., Douglas, D.N., Hao, C., Rinfret, A., Addison, W.R., Fischer, K.P., Churchill, T.A., Lakey, J.R.T., Tyrrell, D.L.J., Kneteman, N.M., 2001. Hepatitis C virus replication in mice with chimeric human livers. Nat. Med. 7, 927–933.

Pietschmann, T., Lohmann, V., Kaul, A., Krieger, N., Rinck, G., Rutter, C., Strand, D., Bartenschlager, R., 2002. Persistent and transient replication of full-length hepatitis C virus genomes in cell culture. J. Virol. 76, 4008–4021.

Randall, G., Rice, C.M., 2001. Hepatitis C virus cell culture replication systems: their potential use for the development of antiviral therapies. Curr. Opin. Infect. Dis. 14, 743–747.

Saito, I., Miyamura, T., Ohbayashi, A., Harada, H., Katayama, T., Kikuchi, S., Watanabe, Y., Koi, S., Onji, M., Ohta, Y., Choo, Q.-L., Houghton, M., Kuo, G., 1990. Hepatitis C virus infection is associated with the development of hepatocellular carcinoma. Proc. Natl. Acad. Sci. USA 87, 6547–6549.

Sugitani, M., Shikata, T., 1998. Comparison of amino acid sequences in hypervariable region-1 of hepatitis C virus clones between human inocula and the infected chimpanzee sera. Virus Res. 56, 177–182.

Takeuchi, K., Boonmar, S., Kubo, Y., Katayama, T., Harada, H., Ohbayashi, A., Choo, Q.-L., Kuo, G., Houghton, M., Saito, I., Miyamura, T., 1990. Hepatitis C virus cDNA clones isolated from a healthy carrier donor implicated in post-transfusion non-A, non-B hepatitis. Gene 91, 287–291.

Takikawa, S., Ishii, K., Aizaki, H., Suzuki, T., Asakura, H., Matsuura, Y., Miyamura, T., 2000. Cell fusion activity of hepatitis C virus envelope proteins. J. Virol. 74, 5066–5074.

Thomson, M., Liang, T.J., 2000. Molecular biology of hepatitis C virus, in: Liang, T.J., Hoofnagle, J.H. (Eds.), Hepatitis C. Academic Press, San Diego, pp. 1–24.

Yanagi, M., Purcell, R.H., Emerson, S.U., Bukh, J., 1997. Transcripts from a single full-length cDNA clone of hepatitis C virus are infectious when directly transfected into the liver of a chimpanzee. Proc. Natl. Acad. Sci. USA 94, 8738–8743.

J Gastroenterol 2004; 39:563–569
DOI 10.1007/s00535-003-1343-0

Journal of Gastroenterology

Methylation status of suppressor of cytokine signaling-1 gene in hepatocellular carcinoma

Hideyuki Miyoshi[1], Hajime Fujie[1], Kyoji Moriya[1], Yoshizumi Shintani[1], Takeya Tsutsumi[1], Masatoshi Makuuchi[2], Satoshi Kimura[1], and Kazuhiko Koike[1]

[1]Department of Internal Medicine, Graduate School of Medicine, University of Tokyo, 7-3-1 Hongo, Bunkyo-ku, Tokyo 113-8655, Japan
[2]Department of Hepatobiliary and Pancreatic Surgery, Graduate School of Medicine, University of Tokyo, Tokyo, Japan

Editorial on page 598

Background. Silencing of the suppressor of cytokine signaling (*SOCS-1*) by aberrant methylation at the CpG island in the coding region gene has been reported in hepatocellular carcinoma (HCC). However, principally, it is methylation in the 5′-noncoding region but not that in the coding region which determines the regulation of gene expression. ***Methods.*** Methylation-specific PCR was performed for the analysis of methylation status both in the 5′-noncoding region and the CpG island of *SOCS-1* from 22 HCC tissue samples with adjacent non-HCC tissue samples and from two cell lines. ***Results.*** Using primers in the CpG island, 9 of 22 HCC samples exhibited aberrant methylation of *SOCS-1*, while only 1 of 22 adjacent non-HCC samples did so. The unmethylation pattern was detected in 1 of 22 HCC and in 5 of 22 non-HCC samples. Thus, aberrant methylation of SOCS-1 was significantly associated with HCC (P = 0.0076 by Fisher's exact test). Using primers in the 5′-noncoding region, aberrant methylation was observed in 12 of 22 HCC and in 2 non-HCC samples. The unmethylated pattern was observed in 5 of 22 HCC and in 10 of 22 non-HCC samples (P = 0.0042). There was no significant correlation between the methylation status of *SOCS-1* and clinicopathological findings, such as the presence or absence of cirrhosis or the histological grade of HCC. ***Conclusions.*** Aberrant methylation of the *SOCS-1* had a significant correlation with HCC. The rate of aberrant methylation was similar in the 5′-noncoding region and in the CpG island. Aberrant methylation of *SOCS-1* may be associated with hepatocarcinogenesis, although further studies are necessary.

Received: July 9, 2003 / Accepted: November 7, 2003
Reprint requests to: K. Koike

Key words: *SOCS-1*, hepatocellular carcinoma, methylation

Introduction

The majority of cases of hepatocellular carcinoma (HCC) are associated with hepatitis B or C viral infection.[1,2] Despite the absence of an appropriate in vitro replication system or a practical infectious animal model system, the mechanism underlying hepatocarcinogenesis in human hepatitis viral infection is on a stable path to elucidation, albeit slowly. Both the direct and indirect effects of hepatitis viruses on HCC development have been shown.[3–6] Accumulation of gene aberrations, such as inactivation of tumor suppressor genes or activation of oncogenes, which may be induced through inflammation-mediated continuous death of hepatocytes followed by regeneration, is considered to be one of the mechanisms underlying hepatocarcinogenesis.[3,4] On the other hand, viral gene products are suggested to contribute to HCC development by their direct effects on hepatocytes.[5–8] Such direct effects have been demonstrated by the use of model systems including mice.[5–7]

In contrast, gene alterations that play pivotal roles in hepatocarcinogenesis in the majority of HCC tissues have not been identified yet. To date, the genes for the APC-axin-GSK-3β complex may be only one of such candidate genes.[9,10] Such gene alterations include not only mutations in the genes per se but also epigenetic changes, which lead to either suppression or augmentation of gene expression. A change in the methylation state of the gene is one of the epigenetic changes that are associated with carcinogenesis. A possible role of methylation of genes in HCC development has been reported[11] for a tumor suppressor gene, $p16^{INK4}$: $p16^{INK4}$ expression was downregulated by methylation of the

control region. Expression of some other cancer-related genes may also be inhibited by methylation.

Silencing of the suppressor of cytokine signaling-1 (SOCS-1; also known as SSI-1 or JAB) is a member of the SOCS protein family. It switches off cytokine signaling by directly interacting with Janus kinase (JAK) proteins; its expression renders cells unresponsive to interleukin-6 stimulation.[12] The SH2 domain of SOCS-1 binds to a JH1 domain of JAK2 and inhibits its phosphorylation, downregulating the JAK/STAT pathway.[12,13] SOCS-1 inhibits the biological effects of cytokines in vivo; its forced expression interrupts macrophage differentiation induced by IL-6 and suppresses CD23 expression induced by IL-4.[12,13] Thus, SOCS-1 modulates the immune system through interacting with the cytokine network.

Recently, *SOCS-1*-deficient mice have been shown to die within 3 weeks after birth from a myeloproliferative disorder resulting from unbridled interferon (IFN)-γ and tumor necrosis factor (TNF)-α signaling.[14] As a negative regulator of cytokine signaling, *SOCS-1* is now a candidate gene for inactivating mutations that will favor the development of malignancies; SOCS-1 may inhibit cell proliferation induced by oncogenic forms of other known SOCS-1-interacting proteins. In addition to the results in hematopoietic neoplasia, recently suppression of SOCS-1 expression has been reported in HCC, in which the CpG-rich domain in the coding region of *SOCS-1* was found to be aberrantly methylated.[15] However, in general, it is the methylation of the 5′ non-coding region, which contains the promoter, but not that of the coding region, which determines gene expression.[16,17] We therefore conducted this experiment to evaluate the methylation status of the *SOCS-1* in HCC by methylation-specific PCR (MSPCR) using primers located both in the 5′-noncoding region and in the CpG-rich domain (CpG island) of the coding region.

Patients and methods

Patients

We studied 22 patients (19 males and 3 females; median age, 63.5 years) with HCC who had underlying chronic hepatitis C with or without cirrhosis (8 without and 14 with cirrhosis), all of whom underwent hepatectomy between 1997 and 2000 at the University of Tokyo Hospital. This study was approved by the ethics review committee of the institute, and carried out in accordance with the World Medical Association Helsinki Declaration, adopted in 1964 and amended in 1996. Informed consent was obtained from each patient. All the patients were positive for anti-hepatitis C virus (HCV) confirmed by the second-generation enzyme immunoassay and HCV-RNA by reverse-transcriptase-polymerase chain reaction (RT-PCR), and none were positive for serum hepatitis B surface antigen (HBsAg). The clinicopathological features of the patients are shown in Table 1.

Tissue samples and cell lines

The cancerous (HCC) and noncancerous (non-HCC) liver tissue samples obtained from these patients were fixed in 10% formalin for hematoxylin and eosin staining, or immediately frozen and stored at −80°C until further use. The histological staging of the noncancerous tissues was performed according to the European classification for chronic hepatitis,[18] and that of cancerous tissue was based on the TNM classification.[19] All the 22 tumors were classified as advanced HCCs: 5 well-, 14 moderately, and 3 poorly differentiated HCCs (see Table 1). Human HCC cell lines PLC/PRF/5, HuH-7, and the B-cell line, BJAB, were obtained from the American Type Culture Collections. The cells were grown in Dulbecco's modified Eagle's medium (DMEM) supplemented with 10% fetal bovine serum.

DNA preparation and bisulfite treatment

Genomic DNA was extracted from the frozen tissues by standard proteinase K digestion and phenol/chloroform extraction.[20] Then, bisulfite modification of genomic DNA was carried out as described previously[21] with slight modification. Briefly, DNA (1 μg) in a volume of 20 μl was denatured by NaOH at a final concentration at 0.3 M for 15 min at 37°C. Then, 113 μl 3.6 M sodium bisulfite (Sigma-Aldrich, St. Louis, MO, USA) at pH 5 and 7.2 μl 10 mM hydroquinone (Sigma-Aldrich), both freshly prepared, were added and mixed well. Then, the samples were incubated under mineral oil at 95°C for 15 min followed by incubation at 50°C for 4 h, and this cycle was repeated 15 times. Modified DNA was purified and resuspended in 50 μl water. The modification was completed by adding NaOH at a final concentration of 0.3 M for 5 min at room temperature, after which ethanol precipitation was carried out.

Genomic and methylation-specific PCR (MSPCR)

Bisulfite-modified and unmodified DNA was subjected to amplification using the PCR method. Primers used for the PCR in the current study are shown in Table 2. Amplification was carried out in a thermal cycler for a total of 35 cycles consisting of 95°C for 30 s, 60°C for 30 s, and 30 s at 72°C in 50 μl reaction mixture containing 200 mM deoxynucleoside triphosphates (dNTPs), 1.0 mM of each primer, and 1× PCR buffer [16.6 mM

Table 1. SOCS-1 gene methylation and clinicopathological findings of 22 hepatocellular carcinoma (HCC) patients

		Methylation of SOCS-1							
		CpG island				5′-noncoding			
		M[a]		U[a]		M[a]		U[a]	
	n	HCC	nHCC	HCC	nHCC	HCC	nHCC	HCC	nHCC
Sex									
Male	19	7	1	1	4	10	2	5	9
Female	3	2	0	0	1	2	0	0	1
Cirrhosis									
−	8	2	0	0	1	3	0	2	4
+	14	7	1	1	4	9	3	3	5
Pathology of HCC[b]									
WD	5	3	0	0	2	3	0	1	3
MD	14	4	1	1	2	7	1	3	6
PD	3	2	0	0	1	2	1	1	0
Tumor size (cm)									
<2	5	2	0	0	0	2	2	2	1
≥2	17	7	1	1	5	10	0	3	9
Vascular invasion									
Absent	19	8	1	1	4	11	2	5	9
Present	3	1	0	0	1	1	0	0	1
Distant metastasis[c]									
M0	20	9	1	1	4	12	1	4	10
M1	2	0	0	0	1	0	1	1	0
Stage grouping[c]									
I	4	1	0	0	0	1	2	2	1
II	5	3	0	0	2	3	0	1	2
III	11	4	1	0	3	6	1	2	7
IV	2	1	0	1	0	2	0	0	0
Overall	22	9* (41%)	1* (5%)	1* (5%)	5* (23%)	12* (55%)	2* (9%)	5* (23%)	10* (46%)

[a] M, hypermethylated pattern; U, unmethylated pattern; not all samples were informative for methylation status
[b] WD, well-differentiated; MD, moderately differentiated; PD, poorly differentiated
[c] According to TNM classification
* $P < 0.01$ when the association of HCC and methylation was judged by Fisher's exact test for each of CpG island and 5′-noncoding region

Table 2. Polymerase chain reaction (PCR) primers used in the current study

	Sequence	Position
Forward		
HM1F	TTCGCGTGTATTTTTAGGTCGGTC	(400–423)
HM2F	GAGTATTCGCGTGTATTTTTAGG	(395–417)
UM1F	TTATGAGTATTTGTGTGTATTTTTAGGTTGGTT	(391–423)
UM2F	TGAGTATTTGTGTGTATTTTTAGG	(394–417)
UMPF-M	GTTCGGTTTCGTTTAGTTTTCGAGG	(−708–684)
UMPF-U	GTTTGGTTTTGTTTAGTTTTTGAGG	(−708–684)
Reverse		
HM1R	CGACACAACTCCTACAACGACCG	(537–559)
UM1R	CACTAACAACACAACTGGTACAACAACCA	(537–565)
UM2R	CAACACAACTCCTACAACAACCA	(543–565)
UMPR-M	ACCCCGACCGACCGCGATCTC	(−590–570)
UMPR-U	ACCCCAACCAACCACAATCTC	(−590–570)

ammonium sulfate, 67 mM Tris-HCl (pH 8.8), 6.7 mM $MgCl_2$, 10 mM 2-mercaptoethanol, and 0.001% (w/v) gelatin] and 1.25 units of Ampli-Taq polymerase (Perkin-Elmer Cetus, Norwalk, CT, USA). The PCR products were separated in a 2.0% agarose gel and visualized by staining with ethidium bromide.

Reverse transcription (RT)-PCR

Total RNA was extracted from cells using RNAzolB (TEL-TEST, Friendswood, TX, USA). Three micrograms of total RNA were reverse transcribed by Superscript II (Gibco-BRL, Gaithersburg, MD, USA) using oligo(dT) primer and subjected to PCR. Primers for RT-PCR of SOCS-1 gene expression were as follows: forward, 5′-CACGCACTTCCGCACATTCC-3′; reverse, 5′-TCCAGCAGCTCGAAGAGGCA-3′. For the RT-PCR, the quantity of cDNA template and the number of amplification cycles were optimized to ensure that the reaction was terminated during the linear phase of product amplification, so that semiquantitative comparisons of the mRNA abundance between different samples were possible. RT-PCR with glyceraldehyde phosphate dihydrogenase (GAPDH) primers was done to adjust the amounts of RNA in each experiment.

Statistical analysis

Fisher's exact test was used for statistical evaluation, and P values below 0.05 were considered significant.

Results

Methylation status of SOCS-1 in cultured cell lines

First, the methylation status of the CpG island in the coding region of *SOCS-1* was analyzed in cell lines by MSPCR using the primer sets, HM1F+HM1R and UM1F+UM1R, according to the method of Yoshikawa et al.[15] MSPCR using these primers, however, could not determine the methylation status of the gene: the use of the primers resulted in dimer formation without methylation- or unmethylation-specific bands. We therefore redesigned new sets of primers located in the CpG island of *SOCS-1* (Table 2; HM2F+HM1R for detecting a methylation-specific band and UM2F+UM2R for an unmethylation-specific band). MSPCR with these sets of primers enabled successful detection of methylation- and unmethylation-specific bands in PLC/PRF/5 cells (Fig. 1). The unmethylation-specific band alone was detected in HuH-7 cells, in agreement with the previous report.[15]

Analysis using the primers located in the 5′-noncoding region (see Table 2) yielded a similar pattern, excluding that there were both methylation- and unmethylation-specific bands also in HuH-7 cells (Fig. 1). Accordingly, the primer sets HM2F+HM1R and UM2F+UM2R were used for the analysis of the methylation status of the CpG island, and UMPF-M+UMPR-M and UMPF-U+UMPR-U were used for the 5′-noncoding region, thereafter.

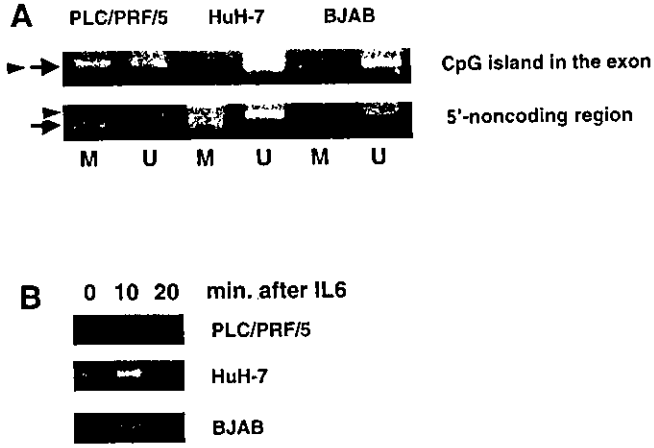

Fig. 1. Genomic and methylation-specific (MSPCR) analysis of cultured hepatoma cell lines in the CpG island and 5′-no-coding region of the *SOCS-1* gene. DNA from human hepatoma cell lines, PLC/PRF/5 and HuH-7, and a B-cell line, BJAB, was analyzed by MSPCR after bisulfite treatment as described in the Patients and methods section. **A** MSPCR with the primers in the CpG island and those in the 5′-noncoding region. **B** RT-PCR showing the expression of SOCS-1 in cell lines before and after the addition of IL-6 (10 ng/ml). The *arrow* indicates the position of the methylation-specific band; the *arrowhead* indicates the position of the unmethylation-specific band. *M*, MSPCR with methylation-specific primers; *U*, MSPCR with unmethylation-specific primers

Expression of SOCS-1 mRNA in cell lines

The expression of SOCS-1 was determined by semiquantitative RT-PCR. Although SOCS-1 expression was abundant in HuH-7 and BJAB cells in the baseline and was enhanced by the addition of IL-6 (10 ng/ml), only marginal expression and no enhancement were detected in PLC/PRF/5 cells. These results are consistent with the methylation status that was determined in the current study and with the expression status in the baseline that was observed in a previous report.[15]

Methylation status of SOCS-1 in human tumor samples

Then, DNA extracted from human HCC and non-HCC tissues was tested for the methylation status of the *SOCS-1* by MSPCR. Only 10 and 6 tissue samples were informative for determining a methylation-specific band